JPET Fast Forward. Published on January 14, 2022 as DOI: 10.1124/jpet.121.000743
This article has not been copyedited and formatted. The final version may differ from this version.

Etavopivat, a Pyruvate Kinase Activator in Red Blood Cells, for the Treatment of Sickle Cell Disease

Patricia Schroeder,[1] Keertik Fulzele,[1] Sanjeev Forsyth, Maria D. Ribadeneira, Sylvie Guichard, Erik Wilker, C. Gary Marshall, Adam Drake, Rose Fessler, Diamantis G. Konstantinidis, Katie G. Seu, and Theodosia A. Kalfa

[1]*Co first authors*

Forma Therapeutics, Watertown, Massachusetts (P.S., K.F.[2], S.F., M.D.R., S.G.); Tango Therapeutics, Cambridge, Massachusetts (E.W.); Repare Therapeutics, Cambridge, Massachusetts (C.G.M.); Ichnos Sciences, Epalinges Switzerland (A.D.); Cincinnati Children's Hospital Medical Center, Cincinnati, Ohio (D.G.K, K.G.S., R.F., T.A.K.); and Department of Pediatrics, College of Medicine, University of Cincinnati, Cincinnati, Ohio (T.A.K.)

[2]*At the time of study conduct*

JPET Fast Forward. Published on January 14, 2022 as DOI: 10.1124/jpet.121.000743
This article has not been copyedited and formatted. The final version may differ from this version.

Running Title: Etavopivat for the treatment of sickle cell disease

Address correspondence to:

Theodosia A. Kalfa

Address: Cincinnati Children's Hospital Medical Center, Cincinnati, Ohio

Tel: 513-636-0989

Fax: 513-636-1330

E mail: Theodosia.Kalfa@cchmc.org

ORCID ID: https://orcid.org/0000-0002-0426-9686

Number of:

Text pages: 31

Figures: 7

References: 52

Supplementary files: 1 text file, 3 tables

Number of words in:

Abstract: 218/ 250

Significance statement: 77/ 80

Introduction: 749/ 750

Discussion: 1344/ 1500

JPET Fast Forward. Published on January 14, 2022 as DOI: 10.1124/jpet.121.000743
This article has not been copyedited and formatted. The final version may differ from this version.

NONSTANDARD ABBREVIATIONS: 2,3-DPG, 2,3-diphosphoglycerate; $AUC_{0–24}$, area under the concentration time curve from time 0–24 hours after dosing; C_{max}; maximum plasma concentration; DMSO, dimethyl sulfoxide; EC_{50}, half maximal effective concentration; EI, elongation index; HbS, hemoglobin S; HbSC, hemoglobin S and C; HbSS, homozygous hemoglobin S; HU, hydroxyurea; LC-MS/MS, liquid chromatography–tandem mass spectrometry; NHP, non-human primate; PD, pharmacodynamic; PK, pharmacokinetic; PKR, erythrocyte pyruvate kinase; pO_2, partial pressure of oxygen; P_{50}, the pO_2 at which hemoglobin is 50% saturated with oxygen; PoS, point of sickling; RBC, red blood cell; SCD, sickle cell disease; TES, N-tris(hydroxymethyl)methyl-2-aminoethanesulfonic acid; VOC, vaso-occlusive crises.

SECTION: Drug Discovery and Translational Medicine

JPET Fast Forward. Published on January 14, 2022 as DOI: 10.1124/jpet.121.000743
This article has not been copyedited and formatted. The final version may differ from this version.

ABSTRACT

Etavopivat is an investigational, oral, small molecule activator of erythrocyte pyruvate kinase (PKR) in development for the treatment of sickle cell disease (SCD) and other hemoglobinopathies. PKR activation is proposed to ameliorate the sickling of SCD red blood cells (RBC) through multiple mechanisms, including reduction of 2,3-diphosphoglycerate (2,3-DPG), which consequently increases hemoglobin (Hb)–oxygen affinity; increased binding of oxygen reduces HbS polymerization and sickling. In addition, PKR activation increases adenosine triphosphate (ATP) produced via glycolytic flux, which helps preserve membrane integrity and RBC deformability. We evaluated the pharmacodynamic response to etavopivat in non-human primates (NHP) and in healthy human subjects, and the effects in RBC from patients with SCD after ex vivo treatment with etavopivat. A single dose of etavopivat decreased 2,3-DPG in NHP and healthy subjects. Hb–oxygen affinity was significantly increased in healthy subjects after 24 hours. Following daily dosing of etavopivat over 5 consecutive days in NHP, ATP was increased by 38% from baseline. Etavopivat increased Hb–oxygen affinity and reduced sickling in RBC collected from SCD patients with either HbSS or HbSC disease. Collectively, these results demonstrate the ability of etavopivat to decrease 2,3-DPG and increase ATP, resulting in increased Hb–oxygen affinity and improved sickle RBC function. Etavopivat is currently being evaluated in clinical trials for the treatment of SCD.

ClinicalTrials.gov identifier: NCT03815695.

JPET Fast Forward. Published on January 14, 2022 as DOI: 10.1124/jpet.121.000743
This article has not been copyedited and formatted. The final version may differ from this version.

SIGNIFICANCE STATEMENT

Etavopivat—a small molecule activator of the glycolytic enzyme erythrocyte pyruvate kinase — decreased 2,3- diphosphoglycerate in red blood cells (RBC) from non-human primates and healthy subjects and significantly increased hemoglobin (Hb)–oxygen affinity in healthy subjects. Using ex vivo RBC from donors with sickle cell disease (SCD) (HbSS or HbSC genotype), etavopivat increased Hb–oxygen affinity and reduced sickling under deoxygenation. Etavopivat shows promise as a treatment for SCD, that potentially might reduce vaso-occlusion and improve anemia.

JPET Fast Forward. Published on January 14, 2022 as DOI: 10.1124/jpet.121.000743
This article has not been copyedited and formatted. The final version may differ from this version.

Introduction

Sickle cell disease (SCD) is an autosomal recessive blood disorder caused by a single point mutation in the *beta globin* gene resulting in the expression of sickle hemoglobin (HbS). HbS tends to polymerize when deoxygenated in the low oxygen tension of capillaries, or even in arterioles. HbS polymerization alters red blood cell (RBC) morphology and negatively affects their function (Sundd et al., 2019). The two most common SCD genotypes are due to homozygosity for the beta-S mutation (p.Glu6Val) (HbSS), or compound heterozygosity for beta-S and beta-C (p.Glu6Lys) (HbSC) (da Guarda et al., 2020). The formation of cytoplasmic HbS polymers causes the RBC to adopt a rigid, sickle-like shape that is the defining characteristic of SCD (Kato et al., 2018). Sickled RBC display abnormal rheological properties, aggregate, and can lead to microcapillary blockage causing tissue hypoxia, which is experienced as a painful vaso-occlusive crisis (VOC). Repeated HbS polymerization and depolymerization with changing oxygen pressure, as well as oxidative damage, alters the RBC membrane, ultimately leading to a significantly shortened RBC lifespan, i.e., hemolysis (Sundd et al., 2019).

Despite increased reticulocyte production, this decreased RBC lifespan results in anemia. The physiologic metabolic response of RBC to anemia is to increase 2,3-DPG, thereby promoting release and offloading of oxygen from hemoglobin (Hb) to tissues. (Charache et al., 1970). This shift to lower oxygen affinity promotes HbS deoxygenation and consequently, polymerization, leading to RBC sickling. Resulting changes in the RBC membrane such as expression of phosphatidyl serine on the cell surface lead to altered interaction with other blood cells and the endothelium. Together with the release of proinflammatory RBC contents upon hemolysis, these changes elicit an inflammatory response, including the activation of white blood cells and increased adhesion of sickle RBC and white blood cells to the endothelium (Telen,

JPET Fast Forward. Published on January 14, 2022 as DOI: 10.1124/jpet.121.000743
This article has not been copyedited and formatted. The final version may differ from this version.

2007), resulting in the sudden, severe, and painful VOC episodes. VOC is the leading diagnosis associated with emergency department visits for patients with SCD (Yusuf et al., 2010); upwards of 40% of such emergency department visits can result in hospital admission (Lanzkron et al., 2010). VOCs also lead to secondary complications, such as acute chest syndrome, that cause end-organ damage and premature death in patients with SCD (Novelli and Gladwin, 2016).

Pyruvate kinase-R (PKR) is the RBC-expressed isoform of the key glycolytic enzyme pyruvate kinase. PKR catalyzes the last and rate-limiting step of glycolysis from phosphoenol-pyruvate to pyruvate while generating adenosine triphosphate (ATP) from adenosine diphosphate. In patients with pyruvate kinase deficiency, decreased PKR activity results in anemia (Zanella et al., 2005), while activation of PKR improves RBC survival and Hb levels (Grace et al., 2019). We hypothesized that PKR activation above normal levels would alter several steps of the glycolytic pathway utilizing glucose to generate pyruvate. Increased PKR activity would be expected to decrease production of 2,3-DPG and increase production of ATP within RBC (Koralkova et al., 2014; Bianchi et al., 2019). PKR is therefore a logical target to activate for treatment of SCD as a decrease in 2,3-DPG levels would increase the affinity of Hb for oxygen, lowering the potential for HbS polymerization and RBC sickling.

Furthermore, an increase in ATP synthesis can enhance overall RBC function and health. Reduced ATP within RBC adversely affects ion homeostasis contributing to cell dehydration (Ortiz et al., 1990; Gallagher, 2017), membrane damage (de Jong et al., 2001; Soupene and Kuypers, 2006; Weiss et al., 2012), and impaired RBC deformability (Clark et al. 1980), all of which contribute to the pathophysiological features of SCD. By attenuating these adverse effects, an increase in ATP synthesis via PKR activation within sickle RBC would potentially have the

JPET Fast Forward. Published on January 14, 2022 as DOI: 10.1124/jpet.121.000743
This article has not been copyedited and formatted. The final version may differ from this version.

dual beneficial effect of addressing the chronic anemia associated with SCD and reducing the incidence of VOC.

Here, we describe the cellular effects of etavopivat (FT-4202), a potent, selective, orally bioavailable PKR activator (Ericsson et al., 2020). Using oral dosing studies in non-human primates (NHP) and healthy subjects, we demonstrate that etavopivat decreases 2,3-DPG and increases ATP in RBC. We also present the results of a series of pharmacodynamic (PD) assays after in vivo treatment of healthy RBCs and ex vivo treatment of sickle RBCs with etavopivat supporting the relevance of these biomarkers when evaluating response to this investigational agent. This work demonstrates the translational value of measurements adopted in preclinical and early clinical development, which are indicative of RBC health. We present target engagement data (single 700-mg dose) from the first-in-human clinical trial that provides a platform of evidence supporting further clinical development of etavopivat for the treatment of SCD.

Materials and Methods

In Vivo Studies

Procedures in Cynomolgus Monkeys. The pharmacokinetics (PK) and PD of etavopivat were assessed in male cynomolgus monkeys. The decision to use male cynomolgus monkeys was based on availability only. There were no PK/PD gender differences observed during preclinical multiple-dose safety studies. Animals (AlphaGenesis, Inc., SC, USA) were of Chinese origin, in good health (non-naïve), and housed, cared for, and acclimated to study procedures in compliance with the testing facility Institutional Animal Care and Use Committee (IACUC) Guidelines and Standard Operating Procedure (Biomere, MA, USA). NHP experiments were

JPET Fast Forward. Published on January 14, 2022 as DOI: 10.1124/jpet.121.000743
This article has not been copyedited and formatted. The final version may differ from this version.

approved by the IACUC at Biomere, MA and conducted according to the National Institutes of Health Guide for the Care and Use of Laboratory Animals (National Research Council, 2011).

A spray-dried dispersion of etavopivat was delivered in a vehicle solution containing 0.5% hydroxypropyl methylcellulose and administered to monkeys by oral gavage. In a single-dose experiment, monkeys (n = 4) received etavopivat at a dose of 50 mg/kg. In a multiple-dose experiment, animals received a dose of 0.5% hydroxypropyl methylcellulose (control; n = 3), or a dose of etavopivat at 3, 8, or 22 mg/kg (n = 4 per group) once daily (QD) on 5 consecutive days. The dose volume for all groups was 5 ml/kg. For the single-dose experiment, whole blood samples (~0.5 ml) for determination of plasma concentrations of etavopivat and whole blood 2,3-DPG and ATP were collected pre-dose, 30 minutes, 1-, 2-, 4-, 6-, 8-, 12-, and 24-hours post-dose. For the multiple-dose experiment, blood samples were collected 1-, 6-, 12-, and 24-hours post-dose on day 1 (~0.5 ml), and pre-dose, 30 minutes, 1-, 2-, 4-, 6-, 8-, 12-, and 24-hours post-dose on day 5 (~0.8 ml).

Single-Dose Plasma PK and PD of Etavopivat in Healthy Subjects. Key aspects of the first-in-human study of etavopivat are summarized below. The study was performed in accordance with the Declaration of Helsinki and Good Clinical Practice guidelines and was approved by the relevant institutional review board. Subjects were healthy volunteers aged 18 to 60 years inclusive and provided written informed consent.

The single-ascending dose portion of the study was a phase 1, single-center, randomized, placebo-controlled, double-blind dose escalation study to assess the safety, tolerability, PK, and PD following a single oral dose of etavopivat in healthy subjects (ClinicalTrials.gov identifier: NCT03815695). Placebo and etavopivat were administered orally to subjects after overnight

JPET Fast Forward. Published on January 14, 2022 as DOI: 10.1124/jpet.121.000743
This article has not been copyedited and formatted. The final version may differ from this version.

fasting. Successively escalated dose levels of etavopivat at 200, 400, 700, and 1000 mg were evaluated. For each sequential dose cohort, eight subjects were randomly assigned 2:6 to receive a single oral dose of placebo or etavopivat, respectively. Blood samples were collected pre- and post-etavopivat dosing at serial timepoints for PK/PD assessment. Etavopivat plasma concentrations were measured using a validated liquid chromatography–tandem mass spectrometry (LC-MS/MS) method. The lower and upper limits of quantitation were 1 and 1000 ng/ml, respectively. 2,3-DPG and ATP in whole blood were measured using a separate LC-MS/MS method as described below. Hb–oxygen affinity and values for the dissolved oxygen pressure (pO_2) at which Hb is 50% saturated with oxygen (P_{50}) were measured in whole blood by generating oxygen equilibrium curves as described below. Non-compartmental PK analysis of etavopivat was conducted using Phoenix WinNonlin® (Certara, Princeton, NJ).

In vitro Studies

Activation of PKR in Human Red Blood Cells. The activation of wild type PKR by etavopivat in mature human RBC ex vivo was evaluated in purified RBC purchased from Research Blood Components (Watertown, MA). Varying concentrations of etavopivat stock solutions (2.5 µl) were added to 22.5 µl of washed human RBC (0.75 million) in the range of 2 nM to 30 µM, in Roswell Park Memorial Institute Medium (Corning; Corning, NY), and incubated for 3 h at 37°C. Cells were spun at 1500 rpm for 5 min and the supernatant was removed. Cells were washed twice using 200 µl of PBS and a 5 min 1500 rpm spin cycle. After the second wash, the RBC pellet was lysed for 30 min in 200 µl of assay buffer. Following a 5 min spin at 1500 rpm, lysate was assayed using a Biovision (Milpitas, CA) Pyruvate Kinase Assay (Catalog # K709-100).

JPET Fast Forward. Published on January 14, 2022 as DOI: 10.1124/jpet.121.000743
This article has not been copyedited and formatted. The final version may differ from this version.

Whole Blood from Patients with SCD. Whole blood samples from female and male patients homozygous for HbS (HbSS), or compound heterozygous for HbS and HbC (HbSC), were collected in vacutainers with K_2-EDTA as an anti-coagulant, at Cincinnati Children's Hospital, with informed consent and in accordance with an Independent Review Board-approved protocol. Whole blood samples (250 µl) from normal control donors (HbAA) and patients with SCD were washed twice with 1 ml Hanks' Balanced Salt Solution (Thermo Fisher Scientific) containing 10 mM HEPES, 10 mM $MgCl_2$, and 5.5 mM glucose at pH 7.4 (Buffer 1) and centrifuged at 400×g for 5 minutes. Supernatant was removed by aspiration. The RBC pellet was resuspended in 1 ml of Buffer 1 and centrifuged for 5 minutes at 800×g to pack the cells. Supernatant was aspirated and packed RBC were resuspended to 20% (v/v) (20% hematocrit) with Buffer 1 and incubated for 4 hours at 37°C with 20 µM etavopivat in dimethyl sulfoxide (DMSO) or equivalent volume of vehicle control (DMSO only) on a VWR Incubating Orbital Shaker 3500 (VWR International, Radnor, PA) at 250 rpm. The concentration of 20 µM etavopivat was selected based on preliminary work showing that this concentration consistently decreased p50 in RBC incubated in vitro with etavopivat for 3 h at 37°C. Hb–oxygen dissociation curves and oxygenscans were performed as described below, to determine P_{50} and point of sickling (PoS), respectively.

Simultaneous Measurement of 2,3-DPG and ATP in Whole Blood. 2,3-DPG and ATP were measured in K_2-EDTA-anticoagulated whole blood samples of monkeys or humans using LC-MS/MS. The analysis was performed using an API-5500 triple-quadrupole mass spectrometer (AB Sciex, Redwood City, CA) coupled with an Agilent 1200 series high-performance liquid chromatography system (Agilent 1260 Infinity Bin Pump and G1379B Degasser, Agilent, Santa

JPET Fast Forward. Published on January 14, 2022 as DOI: 10.1124/jpet.121.000743
This article has not been copyedited and formatted. The final version may differ from this version.

Clara, CA) and a Thermo Scientific CTC-PAL autosampler (Thermo Fisher Scientific, Waltham, MA). Analyst® 1.6.2 (Sciex) and Aria MX software (Thermo Fisher Scientific) were used for instrument control, data acquisition, and data analysis. Calibration standards (25.0–1500 µg/ml), quality controls, and study samples were thawed on wet ice and vortex-mixed for approximately 2 minutes before being pipetted. Because ATP and 2,3-DPG are endogenous molecules present in whole blood at high levels, the low, middle, and high quality control calibration standards were prepared in deionized water (surrogate matrix). Whole blood samples (15 µl) were spiked with stable isotope-labeled internal standard ($^{13}C_{10}$, $^{15}N_5$-ATP, and D_3-2,3-DPG), processed by protein precipitation extraction, and analyzed using ZIC®-pHILIC separation with Turbo Ion Spray® MS/MS detection. Negative $(M-H)^-$ ions for ATP and 2,3-DPG and their respective internal standards, $^{13}C_{10}$, $^{15}N_5$-ATP, and D_3-2, 3-DPG, were monitored in multiple reaction monitoring mode. Analyte to internal standard peak area ratios for the standards were used to create a quadratic calibration curve using $1/x^2$ weighted least-squares regression analysis. For both analytes, the overall accuracy of the method was within ±10.5% (% relative error), and the intra- and inter-assay precision percent coefficient of variation (%CV) were less than 7%.

Hb–Oxygen Dissociation Curve and P_{50} Assessment. The Hb–oxygen equilibrium curves were collected using a TCS HEMOX Analyzer (Guarnone et al., 1995) (TCS Scientific Corp., New Hope, PA) providing the level of oxygenated Hb (expressed as percentage) as a function of pO_2 (mmHg). Whole blood samples from healthy subjects were collected in K_2-EDTA tubes 24 hours after etavopivat treatment. For ex vivo treatment, RBC from patients with SCD were prepared as described above. The whole blood samples or the ex vivo etavopivat-treated RBC were diluted

JPET Fast Forward. Published on January 14, 2022 as DOI: 10.1124/jpet.121.000743
This article has not been copyedited and formatted. The final version may differ from this version.

50-fold into pre-warmed (37^{o}C) TES sodium salt buffer (Sigma Aldrich) containing 20-µl bovine serum albumin-20 additive A and 10-µl anti-foaming agent-25 per 5 ml of buffer.
Samples were oxygenated using compressed air. Measurement using the HEMOX Analyzer (TCS Scientific) started at an oxygen pressure of 145 mmHg following replacement of air with nitrogen and was stopped automatically at an oxygen pressure of 1.9 mmHg. Results were analyzed using the HEMOX Analyzer Software; non-linear regression analysis was performed to obtain the P_{50} value.

Oxygenscan and PoS Calculations. Oxygen gradient ektacytometry (oxygenscan) using a Laser Optical Rotational Red Cell Analyzer (Lorrca®) (RR Mechatronics, Zwaag, The Netherlands) (Rab et al., 2019; Sadaf et al., 2021) was performed to evaluate changes in the deformability of RBC with or without previous etavopivat treatment as a function of oxygen pressure under steady shear stress. 200×10^{6} RBC from patients with SCD treated ex vivo with DMSO or etavopivat, as detailed above, were suspended in 5 ml of Oxy Iso (osmolality 282–286 mOsm/kg, pH 7.35–7.45) at room temperature. The RBC suspension was injected into a rotating wall cylinder maintained at 37°C with a fixed shear stress of 30 pascal. Deoxygenation and reoxygenation of the RBC suspension was achieved by gradual entry of nitrogen gas and ambient air, respectively. One oxygenscan consisted of approximately 80 measurements of the elongation index (EI) during one round of deoxygenation (1300 seconds) and was followed by reoxygenation (280 seconds). Oxygen saturation in the RBC suspension was calculated every 20 seconds based on quenching of the signal using a luminophore oxygen-sensor. Ambient air pO_2 in the cup of the device started at approximately 150 mmHg and was gradually lowered to below 20 mmHg of oxygen. The PoS in oxygenscan is calculated as the pO_2 (mmHg) at which the EI

JPET Fast Forward. Published on January 14, 2022 as DOI: 10.1124/jpet.121.000743
This article has not been copyedited and formatted. The final version may differ from this version.

falls below 5% of the maximum EI (EImax) during deoxygenation and indicates the oxygen pressure at which the polymerization of HbS starts to show effects on RBC deformability.

Statistics

Statistical analysis was performed using Prism, Version 8.4 (GraphPad Software, San Diego, CA). Paired T-test or Wilcoxon tests were used as appropriate. A *P* value less than 0.05 was considered statistically significant for all tests. All preclinical experiments should be considered exploratory. The sample size for the phase 1 study was considered adequate to evaluate the safety, tolerability, and PK/PD of etavopivat; no formal power calculations were performed.

Results

Etavopivat activates PKR in Healthy Human RBC in vitro

The activation of wild type PKR by etavopivat in mature human RBC in vivo was evaluated in purified RBC. Wild type PKR was activated in a concentration-dependent manner. The calculated mean maximum activation was 89% and the half maximal effective concentration (EC_{50}) was 113 nM.

Etavopivat Modulates 2,3-DPG and ATP in Cynomolgus Monkeys

Following the administration of a single 50-mg/kg dose of etavopivat in NHP, the etavopivat plasma concentration reached its maximal value (C_{max}) between 1- and 2-hours post-dose, and 2,3-DPG declined to 47% of the baseline concentration between 12- and 24-hours post-dose (*P*=0.04) (**Fig. 1**), which approaches the theoretical maximum calculated by 2,3-DPG PK/PD

JPET Fast Forward. Published on January 14, 2022 as DOI: 10.1124/jpet.121.000743
This article has not been copyedited and formatted. The final version may differ from this version.

modeling (**Text S1**). Following five consecutive daily doses of etavopivat at lower dose levels (3, 8, and 22 mg/kg), the maximum mean decrease in the concentration of 2,3-DPG occurred 12 hours post-dose on day 1 (**Fig. 2A**), ~12 hours post-etavopivat C_{max} (**Fig. 2B**). The mean concentrations of 2,3-DPG observed on day 5 were comparable to those observed on day 1 (**Fig. 2A**), with mean decreases from baseline of 19% (*P*=0.09), 25% (*P*=0.02), and 36% (*P*=0.002), respectively, 12h after the last dose on day 5.

Due to the temporal delay between etavopivat plasma concentration and 2,3-DPG modulation, direct plots between etavopivat PK and 2,3-DPG response are not meaningful. An indirect PK/PD model, previously applied to describe 2,3-DPG PK/PD relationships (Kha et al., 2015) and described in the supplementary section (**Text S1**), was used to quantitate the exposure-response relationship. This analysis estimates the maximal 2,3-DPG decrease from baseline in NHP with etavopivat is approximately 50%, where the plasma concentration to achieve half of this maximum effect at PK/PD steady state (RC_{50}), a 25% decrease in 2,3-DPG, is ~18 ng/mL (34 nM) from equation 4. Primary PK/PD parameters in NHP are summarized in **Table S1**.

Following a single 50 mg/kg dose, ATP was not significantly elevated from baseline up to 24h post dose. To understand the temporal behavior of ATP elevation upon etavopivat administration, ATP was measured in whole blood from NHP dosed with 3, 8, or 22 mg/kg QD for 5 consecutive days. Concentrations of ATP were not significantly altered at any dose on day 1 (**Fig. 2C)**; however, by day 5, ATP concentrations were elevated at the 8 and 22 mg/kg doses, with day average increases of 18% (*P*=0.0004) and 38% (*P*=0.004), respectively, relative to average levels on day 1. As the dynamics of ATP formation and clearance were not adequately captured, this precluded a quantitative assessment of in vivo EC_{50} for ATP. Etavopivat C_{max} and

JPET Fast Forward. Published on January 14, 2022 as DOI: 10.1124/jpet.121.000743
This article has not been copyedited and formatted. The final version may differ from this version.

area under the concentration time curve from time 0–24 h after dosing ($AUC_{0–24}$) following single and repeated escalating doses in NHP are presented in **Table S2.** Day 5 percent changes of 2,3-DPG and ATP, along with exposure (Day 5 AUC_{0-24}) are summarized in **Fig. 3**.

Ex vivo Etavopivat Treatment of RBC from Patients with SCD Improved Hb–Oxygen Affinity and Reduced PoS

The ability of etavopivat to increase Hb–oxygen affinity in healthy subjects treated with a single dose (**Fig. 4A**) is indicative of the potential to mitigate the rate and extent of RBC sickling in patients with SCD. We tested this possibility ex vivo, using whole blood from donors with either HbSS or HbSC. The p50 in the patients' specimens before the in vitro incubation with vehicle-control or etavopivat was in the range of 28-34 mmHg. Despite optimization of the in vitro incubation media, especially of the buffer composition to maintain as possible stable CO_2 and pH, the p50 values of the sickle red cells incubated under control conditions were relatively lower than baseline as shown in Fig. 4B and C. Nevertheless, etavopivat-incubated RBC under the same conditions as vehicle-control significantly reduced p50. The mean (standard deviation [S.D.]) decrease in P_{50} following treatment with etavopivat versus vehicle was 1.27 ± 0.76 mmHg and 1.47 ± 0.63 mmHg in HbSS and HbSC donors, respectively (**Table S3**). In the HbSS group, P_{50} (mean ± S.D.) was reduced to 24.8 ± 1.82 mmHg after 4-hour incubation with etavopivat compared with 26.1 ± 1.99 mmHg in the vehicle-treated group (*P*=0.0002) (**Fig. 4B**). For the HbSC group, P_{50} was reduced to 24.8 ± 1.58 mmHg after incubation with etavopivat compared with 26.3 ± 1.24 mmHg in the vehicle-treated group (*P*=0.0313) (**Fig. 4C**). Etavopivat treatment induced a leftward shift of the Hb–oxygen dissociation curve in RBC from donors with

JPET Fast Forward. Published on January 14, 2022 as DOI: 10.1124/jpet.121.000743
This article has not been copyedited and formatted. The final version may differ from this version.

either HbSS or HbSC (**Fig. 4D, E**) suggesting an improved oxygen-carrying capacity of Hb under conditions of decreased oxygen pressure.

We tested the deformability of RBC across a pO_2 range, from 150 to <20 mmHg, using oxygen gradient ektacytometry. PoS was calculated as the pO_2 at which RBC maximal deformability (EImax) decreased by 5%. The mean (S.D.) decrease in PoS following incubation with etavopivat for 4 hours versus vehicle was 3.53 ± 4.29 mmHg and 3.91 ± 2.40 mmHg in HbSS and HbSC donors, respectively. Ex vivo incubation of RBC from patients with HbSS with etavopivat decreased the PoS (mean ± S.D.) to 28.3 ± 8.09 mmHg compared with 31.9 ± 7.93 mmHg in the paired samples treated with vehicle control (*P*=0.0244) (**Fig. 5A, C**). PoS was also decreased in etavopivat-treated (19.3 ± 5.11 mmHg) versus vehicle-treated (23.2 ± 5.61 mmHg) RBC from donors with HbSC (*P*=0.0313) (**Fig. 5B, D**).

Human PK of Etavopivat

Following a single oral dose of 700 mg in healthy subjects (one female, five male), etavopivat was rapidly absorbed and median time to maximum concentration was approximately 0.5 hours. After reaching peak concentrations, mean concentrations of etavopivat declined in a multi-exponential manner (**Fig. 6**). The estimated elimination $t_{1/2}$ was approximately 13 hours. Area under the concentration time curve from time 0 extrapolated to infinity (geometric mean [%CV]) was 6995 (29.4) ng·h/ml. Moderate inter-subject variability in plasma etavopivat concentrations was observed.

JPET Fast Forward. Published on January 14, 2022 as DOI: 10.1124/jpet.121.000743
This article has not been copyedited and formatted. The final version may differ from this version.

Etavopivat Decreases 2,3-DPG and Increases Hb–Oxygen Affinity in Healthy Subjects

The PD profile following a single 700-mg dose of etavopivat in healthy subjects was comparable with a single 50-mg/kg dose in NHP. The maximum inhibition of 2,3-DPG was observed 24-hours post-dose, lagging behind the etavopivat C_{max}, which was observed approximately 0.5 hours post-dose. In healthy subjects, concentrations of 2,3-DPG were collected for 7 days following a single 700 mg dose; maximal reductions of 2,3-DPG (mean 49%; p=0.0313) were durable, lasted 48-hours post-dose, and returned to baseline by day 7 (**Fig. 6**). Changes in whole blood concentrations of ATP following a single dose were not significant. Following a single 700-mg dose in healthy subjects, etavopivat was also shown to increase Hb–oxygen affinity (or decrease P_{50}) by 4.85 mmHg at 24 hours, when the greatest decrease in 2,3-DPG was observed (**Table S3**). 2,3-DPG and P_{50} were correlated positively, providing a PKR activation-mediated PD response to etavopivat that increased Hb–oxygen affinity (**Fig. 7**).

Discussion

Advancements in disease-modifying therapies are urgently needed for patients with SCD. Through methodical medicinal chemistry efforts, we have identified etavopivat, a potent, selective, orally bioavailable, and novel PKR activator. Here, we present data from preclinical NHP and early-stage clinical human studies to show that etavopivat decreased 2,3-DPG, and increased ATP in NHP following daily dosing. In RBC from donors with SCD, etavopivat increased Hb–oxygen affinity of RBC and delayed sickling upon deoxygenation. Decreasing the level of deoxygenation that RBCs can tolerate, before sickling, may reduce the incidence of VOC in patients with SCD.

JPET Fast Forward. Published on January 14, 2022 as DOI: 10.1124/jpet.121.000743
This article has not been copyedited and formatted. The final version may differ from this version.

Targeting PKR activation to reduce the concentration of 2,3-DPG is based on the rate-limiting role that PKR plays in regulating glycolysis in RBC. A decrease in 2,3-DPG with PKR activation has been demonstrated in preclinical studies, in healthy subjects, and in patients with PKR deficiency after treatment (Chubukov et al., 2016; Kung et al., 2017; Yang et al., 2019). Decreases in 2,3-DPG in both NHP and humans were delayed relative to peak plasma concentrations of etavopivat. More specifically, in NHP, maximum decreases in whole blood 2,3-DPG were observed between 12- and 24-hours post-dose, sometime after the mean C_{max} was achieved, typically 1-hour post-dose. A comparable observation was made following a single 700-mg dose in healthy subjects. Notably, the maximal decrease in 2,3-DPG in healthy subjects treated with a single 700 mg dose of etavopivat was durable for 48 hours before slowly returning to baseline by day 7. Following a single dose, maximum decreases in 2,3-DPG in NHP dosed with 50 mg/kg and healthy human subjects treated with 700 mg was 47% and 49%, respectively, consistent with comparable unbound exposure at those dose levels (2342 and 2099 ng/ml*h for NHP and humans, respectively). Mitigating 2,3-DPG has been proposed as a means to reduce HbS polymerization in patients with SCD (Eaton and Bunn, 2017). Basal concentrations of 2,3-DPG are higher in patients with SCD compared with healthy controls (Charache et al., 1970; Castro, 1980; Ould Amar et al., 1996), and depletion of 2,3-DPG has been shown to reduce the tendency for RBC sickling in patients with SCD (Poillon et al., 1995).

2,3-DPG strongly influences the binding of oxygen to Hb; by binding within the central cavity of the Hb tetramer, 2,3-DPG causes allosteric changes, and reduces the molecule's affinity to oxygen (MacDonald, 1977). Increased Hb–oxygen affinity (decreased P_{50}) with a mean delta P_{50} of 4.85 mmHg was observed in healthy subjects following the administration of a single 700-

JPET Fast Forward. Published on January 14, 2022 as DOI: 10.1124/jpet.121.000743
This article has not been copyedited and formatted. The final version may differ from this version.

mg dose of etavopivat. P_{50} and 2,3-DPG in blood were strongly correlated before and 24 hours following a single dose of etavopivat. The 2,3-DPG-mediated effect provides a PD-based rationale for the increased Hb–oxygen affinity after treatment with etavopivat. Furthermore, ex vivo experiments using RBC from donors with HbSS or HbSC showed decreases in P_{50}, indicating increased Hb–oxygen affinity in the presence of etavopivat. Since higher concentrations of 2,3-DPG are associated with increases in deoxy-Hb, therapeutic approaches that increase Hb–oxygen affinity and consequently reduce deoxygenation of HbS, are expected to decrease HbS polymerization, reduce sickling, and attenuate the clinical consequences of SCD.

In addition to the reduction in 2,3-DPG and associated improvement in Hb–oxygen affinity, the increased glycolytic flux induced by PKR activation is expected to increase RBC function and health by increasing ATP and reducing oxidative stress. Although no meaningful elevation in ATP was observed following a single dose in monkeys or healthy subjects, ATP concentrations were elevated by as much as 38% (P=0.004) relative to day 1 in NHP following 5 consecutive days of QD doses of etavopivat. In a recent study in Berkeley sickle cell anemia mice, ATP levels were increased (P<0.01) following two weeks of treatment with etavopivat, corresponding with etavopivat plasma levels of 7702 ± 796 ng/mL (Shrestha et al., 2021). ATP plays an essential role in maintenance of RBC membrane-cytoskeletal integrity (Betz et al., 2009), membrane repair via activation of flippase to re-internalize phosphatidyl serine to the inner leaflet of the RBC membrane (Soupene and Kuypers, 2006; Weiss et al., 2012), cell hydration (Gallagher, 2017), maintenance of ionic (Mg^{2+} and Ca^{2+}) gradients (Ortiz et al. 1990; Raftos et al., 1999; Rivera et al., 2005), RBC deformability (Weed et al., 1969; McMahon, 2019), and protection from oxidative damage (Banerjee and Kuypers, 2004). Therefore,

JPET Fast Forward. Published on January 14, 2022 as DOI: 10.1124/jpet.121.000743
This article has not been copyedited and formatted. The final version may differ from this version.

increasing ATP concentrations is likely to have broad beneficial effects for patients with SCD. Moreover, in the current study, ex vivo treatment with etavopivat significantly improved the PoS in the RBC from donors with the HbSS genotype, likely due to a reduction in 2,3-DPG. These dual effects of decreased 2,3-DPG and increased ATP suggest that etavopivat has the potential to reduce RBC sickling, hemolysis, anemia, and consequently, VOC.

Pharmacologic interventions in clinical practice or development for the treatment of SCD include approaches to increase fetal Hb or Hb oxygenation in order to decrease Hb polymerization, and to decrease vascular adhesion. The current standard of care for most patients with SCD is hydroxyurea (HU), which reduces sickling by increasing fetal Hb in RBC and reduces painful episodes of VOC by ~50%; however, the effectiveness of HU can be confounded by poor patient compliance and discontinuation rates can be high (Brandow and Panepinto, 2010; Agrawal et al., 2014; Shah et al., 2019). In addition, while HU is broadly efficacious, response to treatment can be variable, and a proportion of patients (10–20%) are non-responsive (Steinberg et al., 1997; Ma et al., 2007; Steinberg, 2008). Furthermore, HU is a myelosuppressive agent that may cause neutropenia and thrombocytopenia and thus requires routine blood monitoring for side effects (Agrawal et al., 2014). While HU has been used to treat SCD for over 30 years, there remains a need for improved disease management, more pharmacological options, and the possibility of combination therapies to target different aspects of SCD pathology. Crizanlizumab was recently approved to reduce the frequency of VOC in adults and pediatric patients aged 16 years and older with SCD. However, no improvement in hemolysis, anemia, or markers of inflammation have been observed (Ataga et al., 2017; Blair, 2020a). These data suggest that although targeting endothelial adhesion may decrease the incidence and severity of VOC, these agents are unlikely to address the anemia or chronic tissue damage associated with SCD. Drugs

JPET Fast Forward. Published on January 14, 2022 as DOI: 10.1124/jpet.121.000743
This article has not been copyedited and formatted. The final version may differ from this version.

that increase Hb–oxygen affinity, such as the recently approved agent voxelotor, directly interfere with HbS polymerization by maintaining a higher proportion of Hb in oxygenated state (Vichinsky et al., 2019; Blair, 2020b). Although the clinical safety profile for voxelotor to date has been positive, there is a recognized risk that excessive oxygen affinity could cause hypoxia by preventing release of oxygen into tissues, for which routine neurovascular monitoring has been recommended (Hebbel and Hedlund, 2017). Activation of PKR follows a physiological pathway that increases Hb–oxygen affinity by decreasing 2,3-DPG and is likely to counteract the pathophysiology of SCD while enabling oxygen release in hypoxic tissues. As a result of the combination of decreased 2,3-DPG and increased ATP, it is proposed that targeting PKR activation may have a broad and significant impact on SCD, both in HbSS and HbSC, by improving the membrane integrity of RBC.

In conclusion, by virtue of its ability to promote activity in the glycolytic pathway, etavopivat is hypothesized to have unique, beneficial, disease-modifying effects on SCD. As the enzyme that catalyzes the last step of glycolysis, PKR underpins reactions that directly impact the metabolic health and primary functions of RBC. Etavopivat has two key effects: first, it decreases 2,3-DPG, which can reduce HbS polymerization and potentially attenuate clinical sequela of vaso-occlusion in SCD, and second, it increases ATP, which provides metabolic resources to support membrane integrity and protect against the loss of RBC deformability, and potentially to mitigate hemolysis in patients with SCD. The PD response to etavopivat in relation to PKR was demonstrated pre-clinically and confirmed in the first-in-human trial, providing valuable evidence of target modulation, which supports the rationale for subsequent clinical trials. Furthermore, the preliminary safety profile of etavopivat supports its advancement to

JPET Fast Forward. Published on January 14, 2022 as DOI: 10.1124/jpet.121.000743
This article has not been copyedited and formatted. The final version may differ from this version.

additional clinical trials to determine the risk/benefit profile of PKR activation in SCD. Clinical trials of etavopivat in patients with SCD are currently in progress.

Acknowledgments

The authors would like to thank Dr Frans Kuypers for helpful discussions and Dr Eric Wu for his contribution to statistical analyses. Medical writing assistance was provided by Sue Reinwald, PhD, and Katy Beck, PhD, of Engage Scientific Solutions, Horsham, UK, and was funded by Forma Therapeutics, Inc.

Authorship Contributions

Participated in research design: Schroeder, Fulzele, Kalfa, Seu, Konstantinidis, Drake, Wilker, Marshall, Guichard, Forsyth, Ribadeneira

Conducted experiments*:* Fessler, Konstantinidis, Seu, Ribadeneira

Contributed new reagents or analytic tools: Konstantinidis, Seu

Performed data analysis: Schroeder, Fulzele, Guichard, Kalfa, Seu, Konstantinidis, Fessler, Forsyth, Ribadeneira

Wrote or contributed to the writing of the manuscript: Schroeder, Fulzele, Forsyth, Ribadeneira, Guichard, Wilker, Marshall, Drake, Kalfa, Seu, Konstantinidis, Fessler

Declaration of Interests

JPET Fast Forward. Published on January 14, 2022 as DOI: 10.1124/jpet.121.000743
This article has not been copyedited and formatted. The final version may differ from this version.

PS, SG SF, and MDR are employees of Forma Therapeutics and may own shares in Forma Therapeutics.

KF is a previous employee of Forma Therapeutics and reports equity ownership.

AD is a previous employee of Forma Therapeutics and owns shares in Forma Therapeutics.

TAK receives research funding from Forma Therapeutics and from Agios Pharmaceuticals and honoraria from Agios Pharmaceuticals for participation in Steering Committee.

KGS, DK, GM, EW, and RF have nothing to declare.

JPET Fast Forward. Published on January 14, 2022 as DOI: 10.1124/jpet.121.000743
This article has not been copyedited and formatted. The final version may differ from this version.

References

Agrawal RK, Patel RK, Shah V, Nainiwal L, and Trivedi B (2014) Hydroxyurea in sickle cell disease: drug review. *Indian J Hematol Blood Transfus* **30**:91-96.

Ataga KI, Kutlar A, Kanter J, Liles D, Cancado R, Friedrisch J, Guthrie TH, Knight-Madden J, Alvarez OA, Gordeuk VR, Gualandro S, Colella MP, Smith WR, Rollins SA, Stocker JW, and Rother RP (2017) Crizanlizumab for the prevention of pain crises in sickle cell disease. *N Engl J Med* **376**:429-439.

Banerjee T and Kuypers FA (2004) Reactive oxygen species and phosphatidylserine externalization in murine sickle red cells. *Br J Haematol* **124**:391-402.

Betz T, Lenz M, Joanny JF, and Sykes C (2009) ATP-dependent mechanics of red blood cells. *Proc Natl Acad Sci U S A* **106**:15320-15325.

Bianchi P, Fermo E, Glader B, Kanno H, Agarwal A, Barcellini W, Eber S, Hoyer JD, Kuter DJ, Maia TM, Mañu-Pereira MDM, Kalfa TA, Pissard S, Segovia JC, van Beers E, Gallagher PG, Rees DC, and van Wijk R (2019) Addressing the diagnostic gaps in pyruvate kinase deficiency: consensus recommendations on the diagnosis of pyruvate kinase deficiency. *Am J Hematol* **94**:149-161.

Blair HA (2020a) Crizanlizumab: first approval. *Drugs* **80**:79-84.

Blair HA (2020b) Voxelotor: first approval. *Drugs* **80**:209-215.

Brandow AM and Panepinto JA (2010) Hydroxyurea use in sickle cell disease: the battle with low prescription rates, poor patient compliance and fears of toxicities. *Expert Rev Hematol* **3**:255-260.

Castro O (1980) Viability and function of stored sickle erythrocytes. *Transfusion* **20**:695-703.

Charache S, Grisolia S, Fiedler AJ, and Hellegers AE (1970) Effect of 2,3-diphosphoglycerate on oxygen affinity of blood in sickle cell anemia. *J Clin Invest* **49**:806-812.

Chubukov V, Johnson K, Kosinski P, Clasquin M, Jha A, Kim H, Roddy T, Merica E, Barbier A, Dang L, Silverman L, and Kung C (2016) Characterization of metabolic response to AG-348, an allosteric activator of red cell pyruvate kinase, in healthy volunteers and pyruvate kinase deficiency patients. *Blood* **128**:2452.

Clark MR, Mohandas N, and Shohet SB (1980) Deformability of oxygenated irreversibly sickled cells. *J Clin Invest* **65**:189-196.

da Guarda CC, Yahouédéhou S, Santiago RP, Neres J, Fernandes CFL, Aleluia MM, Figueiredo CVB, Fiuza LM, Carvalho SP, Oliveira RM, Fonseca CA, Ndidi US, Nascimento VML, Rocha LC, and Goncalves MS (2020) Sickle cell disease: a distinction of two most frequent genotypes (HbSS and HbSC). *PLoS One* **15**:e0228399.

Dayneka NL, Garg V, and Jusko WJ (1993) Comparison of four basic models of indirect pharmacodynamic responses. *J Pharmacokinet Biopharm* **21**: 457-478.

de Jong K, Larkin SK, Styles LA, Bookchin RM, and Kuypers FA (2001) Characterization of the phosphatidylserine-exposing subpopulation of sickle cells. *Blood* **98**:860-867.

Eaton WA and Bunn HF (2017) Targeting sickle cell disease by targeting HbS polymerization. *Blood* **129**:2719-2726.

Ericsson A, Green N, Gustafson G, Lancia DR. Jr, Marshall G, Mitchell L, Richard D, Wang Z, Forsyth S, Kelly PJ, Mondal M, Ribadeneira M, and Schroeder P (2020) Treating sickle cell disease with a pyruvate kinase R activating compound. United States Patent Number 10,675,274. Patent Images (uspto.gov). Accessed June 8, 2021.

Gallagher P (2017) Disorders of erythrocyte hydration. *Blood* **130**:2699-2708.

Grace RF, Layton DM, and Barcellini W (2019) How we manage patients with pyruvate kinase deficiency. *Br J Haematol* **184**:721-734.

Guarnone R, Centenara E, and Barosi G (1995) Performance characteristics of Hemox-Analyzer for assessment of the hemoglobin dissociation curve. *Haematologica* **80**:426-430.

Hebbel RP and Hedlund BO (2017) Sickle hemoglobin oxygen affinity-shifting strategies have unequal cerebrovascular risks. *Am J Hematol* **93**:321-325.

Kato GJ, Piel FB, Reid CD, Gaston MH, Ohene-Frempong K, Krishnamurti L, Smith WR, Panepinto JA, Weatherall DJ, Costa FF, and Vichinsky EP (2018) Sickle cell disease. *Nat Rev Dis Primers* **4**:18010.

Kha L, Cohen M, Chen Y, Kim H, Silver B, Agresta S, Merica E, Kung C, Kosinski P, Silverman L, Biller S, and Yang H (2015) Population pharmacokinetics and pharmacodynamics of AG-348 in healthy human volunteers guide dose selection for the treatment of pyruvate kinase deficiency. *Blood* **126**:3336.

Koralkova P, van Solinge WW, and van Wijk R (2014) Rare hereditary red blood cell enzymopathies associated with hemolytic anemia - pathophysiology, clinical aspects, and laboratory diagnosis. *Int J Lab Hematol* **36**:388-397.

Kung C, Hixon J, Kosinski PA, Cianchetta G, Histen G, Chen Y, Hill C, Gross S, Si Y, Johnson K, DeLaBarre B, Luo Z, Gu Z, Yao G, Tang H, Fang C, Xu Y, Lv X, Biller S, Su SM, Yang H, Popovici-Muller J, Salituro F, Silverman L, and Dang L (2017) AG-348 enhances pyruvate kinase activity in red blood cells from patients with pyruvate kinase deficiency. *Blood* **130**:1347-1356.

Lanzkron S, Carroll CP, and Haywood C, Jr. (2010) The burden of emergency department use for sickle-cell disease: an analysis of the national emergency department sample database. *Am J Hematol* **85**:797-799.

Ma Q, Wyszynski DF, Farrell JJ, Kutlar A, Farrer LA, Baldwin CT, and Steinberg MH (2007) Fetal hemoglobin in sickle cell anemia: genetic determinants of response to hydroxyurea. *Pharmacogenomics J* **7**:386-394.

MacDonald R (1977) Red cell 2,3-diphosphoglycerate and oxygen affinity. *Anaesthesia* **32**:544-553.

McMahon TJ (2019) Red blood cell deformability, vasoactive mediators, and adhesion. *Front Physiol* **10**:1417.

National Research Council (US) Committee for the Update of the Guide for the Care and Use of Laboratory Animals. (2011). Guide for the Care and Use of Laboratory Animals, 8th edition. National Academies Press, Washington, D.C.

Novelli EM and Gladwin MT (2016) Crises in sickle cell disease. *Chest* **149**:1082-1093.

Ortiz OE, Lew VL, and Bookchin RM (1990) Deoxygenation permeabilizes sickle cell anaemia red cells to magnesium and reverses its gradient in the dense cells. *J Physiol* **427**:211-226.

Ould Amar AK, Kerob-Bauchet B, Robert P, Leconte C, Maier H, Bera O, Plumelle Y, Hyronimus JC, and Césaire R (1996) Assessment of qualitative functional parameters of stored red blood cells from donors with sickle cell trait (AS) or with heterozygote (AC) status. *Transfus Clin Biol* **3**:225-233.

Poillon WN, Kim BC, Labotka RJ, Hicks CU, and Kark JA (1995) Antisickling effects of 2,3-diphosphoglycerate depletion. *Blood* **85**:3289-3296.

Rab MAE, van Oirschot BA, Bos J, Merkx TH, van Wesel ACW, Abdulmalik O, Safo MK, Versluijs BA, Houwing ME, Cnossen MH, Riedl J, Schutgens REG, Pasterkamp G, Bartels M, van Beers EJ, and van Wijk R (2019) Rapid and reproducible characterization of sickling during automated deoxygenation in sickle cell disease patients. *Am J Hematol* **94**:575-584.

Raftos JE, Lew VL, and Flatman PW. Refinement and evaluation of a model of Mg2+ buffering in human red cells (1999) *Eur J Biochem* **263**:635-645.

Rivera A, Ferreira A, Bertoni D, Romero JR, and Brugnara C (2005) Abnormal regulation of Mg2+ transport via Na/Mg exchanger in sickle erythrocytes. *Blood* **105**:382-386.

Sadaf A, Seu KG, Thaman E, Fessler R, Konstantinidis DG, Bonar HA, Korpik J, Ware RE, McGann PT, Quinn CT, and Kalfa TA. (2021) Automated Oxygen Gradient Ektacytometry: A Novel Biomarker in Sickle Cell Anemia. *Front Physiol* **12**:636609.

Shah N, Bhor M, Xie L, Halloway R, Arcona S, Paulose J, and Yuce H (2019) Treatment patterns and economic burden of sickle-cell disease patients prescribed hydroxyurea: a retrospective claims-based study. *Health Qual Life Outcomes* **17**:155.

Sharma A, and Jusko WJ (1998) Characteristics of indirect pharmacodynamic models and applications to clinical drug responses. *Br J Clin Pharmacol* **45**:229-239.

Shrestha A, Chi M, Wagner K, Malik A, Korpik J, Drake A, Fulzele K, Guichard S, and Malik P (2021) FT-4202, an oral PKR activator, has potent antisickling effects and improves RBC survival and Hb levels in SCA mice. *Blood Adv* **5**: 2385-2390.

Soupene E and Kuypers FA. Identification of an erythroid ATP-dependent aminophospholipid transporter (2006) *Br J Haematol* **133**:436-438.

Steinberg MH, Lu ZH, Barton FB, Terrin ML, Charache S, and Dover GJ (1997) Fetal hemoglobin in sickle cell anemia: determinants of response to hydroxyurea. Multicenter Study of Hydroxyurea. *Blood* **89**:1078-1088.

Steinberg MH (2008) Sickle cell anemia, the first molecular disease: overview of molecular etiology, pathophysiology, and therapeutic approaches. *ScientificWorldJournal* **8**:1295-1324.

Sundd P, Gladwin MT, and Novelli EM (2019) Pathophysiology of sickle cell disease. *Annu Rev Pathol* **14**:263-292.

Telen MJ (2007) Role of adhesion molecules and vascular endothelium in the pathogenesis of sickle cell disease. *Hematology Am Soc Hematol Educ Program*:84-90.

Vichinsky E, Hoppe CC, Ataga KI, Ware RE, Nduba V, El-Beshlawy A, Hassab H, Achebe MM, Alkindi S, Brown RC, Diuguid DL, Telfer P, Tsitsikas DA, Elghandour A, Gordeuk VR, Kanter J, Abboud MR, Lehrer-Graiwer J, Tonda M, Intondi A, Tong B, Howard J, and Investigators HT (2019) A phase 3 randomized trial of voxelotor in sickle cell disease. *N Engl J Med* **381**:509-519.

Weed RI, LaCelle PL, and Merrill EW (1969) Metabolic dependence of red cell deformability. *J Clin Invest* **48**:795-809.

Weiss E, Cytlak UM, Rees DC, Osei A, and Gibson JS (2012) Deoxygenation-induced and Ca(2+) dependent phosphatidylserine externalisation in red blood cells from normal individuals and sickle cell patients. *Cell Calcium* **51**:51-56.

Yang H, Merica E, Chen Y, Cohen M, Goldwater R, Kosinski PA, Kung C, Yuan ZJ, Silverman L, Goldwasser M, Silver BA, Agresta S, and Barbier AJ (2019) Phase 1 single- and multiple-ascending-dose randomized studies of the safety, pharmacokinetics, and

pharmacodynamics of AG-348, a first-in-class allosteric activator of pyruvate kinase R, in healthy volunteers. *Clin Pharmacol Drug Dev* **8**:246-259.

Yusuf HR, Atrash HK, Grosse SD, Parker CS, and Grant AM (2010) Emergency department visits made by patients with sickle cell disease: a descriptive study, 1999-2007. *Am J Prev Med* **38**:S536-S541.

Zanella A, Fermo E, Bianchi P, and Valentini G (2005) Red cell pyruvate kinase deficiency: molecular and clinical aspects. *Br J Haematol* **130**:11-25.

JPET Fast Forward. Published on January 14, 2022 as DOI: 10.1124/jpet.121.000743
This article has not been copyedited and formatted. The final version may differ from this version.

Unnumbered Footnotes

This study was funded by Forma Therapeutics, Inc., Watertown, MA.

Pharmacokinetic data from healthy subjects following a single dose of etavopivat was previously presented at the European Hematology Association Annual Congress, 2020 (Estepp JH et al, Hemasphere, 2020, 4, 709-710).

Reprint requests to:
Theodosia A. Kalfa,
Address: Cincinnati Children's Hospital Medical Center, Cincinnati, Ohio
Tel: 513-636-0989
Fax: 513-636-1330
E mail: Theodosia.Kalfa@cchmc.org

Numbered Footnotes

[1]Co first authors
[2]At the time of study conduct

JPET Fast Forward. Published on January 14, 2022 as DOI: 10.1124/jpet.121.000743
This article has not been copyedited and formatted. The final version may differ from this version.

[[Figure Legends]]

Fig. 1. Relationship between the PK of etavopivat and the PD of 2,3-DPG in non-human primates. PK profiles of NHP (*n* = 4) administered a single 50-mg/kg dose of etavopivat demonstrated rapid absorption and mean C_{max} of 1823 ng/ml etavopivat and an AUC_{0-24} of 8877 ng/mL*h (AUC_{0-inf} = 9007 ng/mL*h). At this dose level, 2,3-DPG decreased by an average of 47% between 12 and 24h post dose versus baseline (paired T-test; *P*=0.04). Data are expressed as mean ± S.D.

2,3-DPG, 2,3-diphosphoglycerate; $AUC_{0–inf}$, area under the concentration time curve from time 0–infinity; C_{max}; maximum plasma concentration; NHP, non-human primate; PD, pharmacodynamics; PK, pharmacokinetics; S.D., standard deviation.

Fig. 2. Dose-response time course modulation of 2,3-DPG and ATP following 5 consecutive days of QD dosing of etavopivat in non-human primates. *N* = 4 per treatment group. For all graphs, data are expressed as mean ± S.D. and analyzed using paired T-tests (2,3-DPG, baseline vs 12h post last dose on Day 5; ATP, Day 1 vs Day 5). (Panel A) Blood 2,3-DPG profile on day 1 and day 5 of consecutive QD dosing of 3, 8, or 22 mg/kg. (Panel B) Plasma PK profile of etavopivat on day 1 and day 5 of consecutive QD dosing of 3, 8, or 22 mg/kg. (Panel C) Blood ATP profile on day 1 and day 5 of consecutive QD dosing of 3, 8, or 22 mg/kg.

2,3-DPG, 2,3-diphosphoglycerate; ATP, adenosine triphosphate; PK, pharmacokinetic; QD, once daily; S.D., standard deviation.

Fig. 3. Day 5 percent changes in 2,3-DPG and ATP, along with exposure (Day 5 AUC_{0-24}) following 5 consecutive days of QD dosing of etavopivat in non-human primates. *N* = 4 per

JPET Fast Forward. Published on January 14, 2022 as DOI: 10.1124/jpet.121.000743
This article has not been copyedited and formatted. The final version may differ from this version.

etavopivat treatment group and *N* = 3 for the placebo group. Data plotted are mean ± S.D, analyzed using paired T-tests. **P*<0.05; ***P*<0.01; ****P*<0.001. Day 5 $AUC_{0\text{-}24}$ data are mean (S.D.).

2,3-DPG, 2,3-diphosphoglycerate; ATP, adenosine triphosphate; $AUC_{0–24}$, area under the concentration time curve from time 0–24 hours after dosing QD, once daily; S.D., standard deviation.

Fig. 4. Etavopivat improves the Hb–oxygen dissociation curve in healthy subjects and in RBC from sickle cell donors with HbSS and HbSC disease. Treatment with etavopivat significantly decreased the P_{50} of healthy subjects treated with a single dose of etavopivat (*n* = 6) (Panel A). Isolated RBC from HbSS or HbSC donors were treated ex vivo with either 20 µM etavopivat or DMSO (vehicle) for 4 hours at 37°C. Treatment with etavopivat significantly decreased the P_{50} in RBCs from both HbSS (*n* = 13; Panel B) and HbSC (*n* = 6; Panel C) donors. Representative oxygen equilibrium curves are shown for HbSS (Panel D) and HbSC (Panel E). Data were analyzed using non-parametric Wilcoxon matched-pairs signed rank test. **P*<0.05; ****P*<0.001. Hb, hemoglobin; HbSC, hemoglobin SC; HbSS, hemoglobin SS; HS, healthy subjects; P_{50}, the dissolved oxygen pressure at which Hb−oxygen-binding is 50% saturated; RBC, red blood cells; SAD, single-ascending dose; SCD, sickle cell disease.

Fig. 5. Etavopivat reduced the dissolved oxygen pressure at which HbSS or HbSC RBC initiate sickling. Isolated RBC from donors with either HbSS or HbSC genotype were treated ex vivo with either 20 µM etavopivat or DMSO (vehicle) for 4 hours at 37°C. Curves for RBC deformability as a function of dissolved oxygen pressure (oxygenscan) were constructed using

JPET Fast Forward. Published on January 14, 2022 as DOI: 10.1124/jpet.121.000743
This article has not been copyedited and formatted. The final version may differ from this version.

Lorrca®. The PoS at which the deformation of RBC reached 5% from baseline was calculated and plotted. Treatment with etavopivat significantly decreased the PoS in RBCs from both HbSS (*n* = 11; Panel A) and HbSC (*n* = 6; Panel B) donors. Representative oxygenscans for RBCs from a HbSS donor (Panel C) and a HbSC donor (Panel D) are shown. Data were analyzed using the non-parametric Wilcoxon matched-pairs signed rank test. **P*<0.05.

DMSO, dimethyl sulfoxide; HbSC, hemoglobin SC; HbSS, hemoglobin SS; PoS, point of sickling; RBC, red blood cells; SCD, sickle cell disease.

Fig. 6. Relationship between the PK of etavopivat and the PD of 2,3-DPG in healthy human subjects. PK profiles in healthy subjects (*n* = 6) administered 700 mg of etavopivat demonstrated rapid absorption and mean C_{max} of 2204 ng/ml and $AUC_{0\text{-}inf}$ of 6995 ng·h/ml. PD analysis of 2,3-DPG in the same subjects demonstrated maximum reductions at 24 hours with durable reductions of 2,3-DPG of 48% through 48 hours and a return to baseline by day 7 (Panel A). Panel B is presented to show greater clarity at early timepoints (0–24 hours). Data are mean ± S.D. at each time point.

2,3-DPG, 2,3-diphosphoglycerate; $AUC_{0–inf}$, area under the concentration time curve from time 0–infinity; C_{max}; maximum plasma concentration; PD, pharmacodynamic; PK, pharmacokinetic; S.D., standard deviation.

Fig. 7. Relationship between 2,3-DPG and P_{50} in healthy subjects following a single 700-mg dose of etavopivat. Hb−oxygen affinity shifts were measured in the blood of healthy subjects (*n* = 6) prior to dosing etavopivat and at 24 hours post-dose, coinciding with an increased Hb−

JPET Fast Forward. Published on January 14, 2022 as DOI: 10.1124/jpet.121.000743
This article has not been copyedited and formatted. The final version may differ from this version.

oxygen affinity (a decrease in P_{50}) that was positively correlated with decreases in the mean blood concentrations of 2,3-DPG.

2,3-DPG, 2,3-diphosphoglycerate; Hb, hemoglobin; P_{50}, the partial pressure of dissolved oxygen at which Hb is 50% saturated with oxygen.

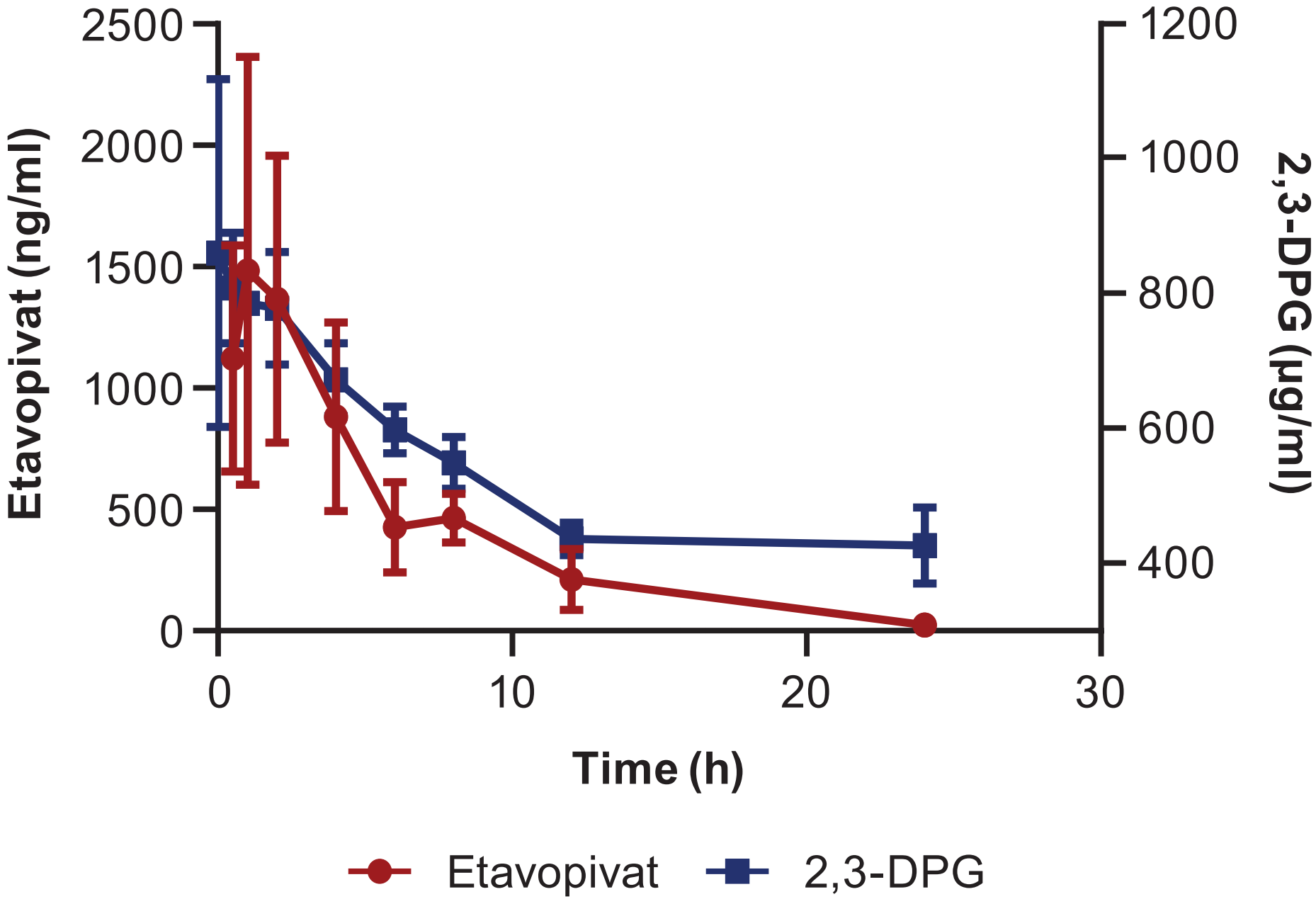
2500
2000
1500
1000
500
0
Etavopivat (ng/ml)
1200
1000
800
600
400
2,3-DPG (µg/ml)
0
10
20
30
Time (h)
Etavopivat
2,3-DPG

Figure 1

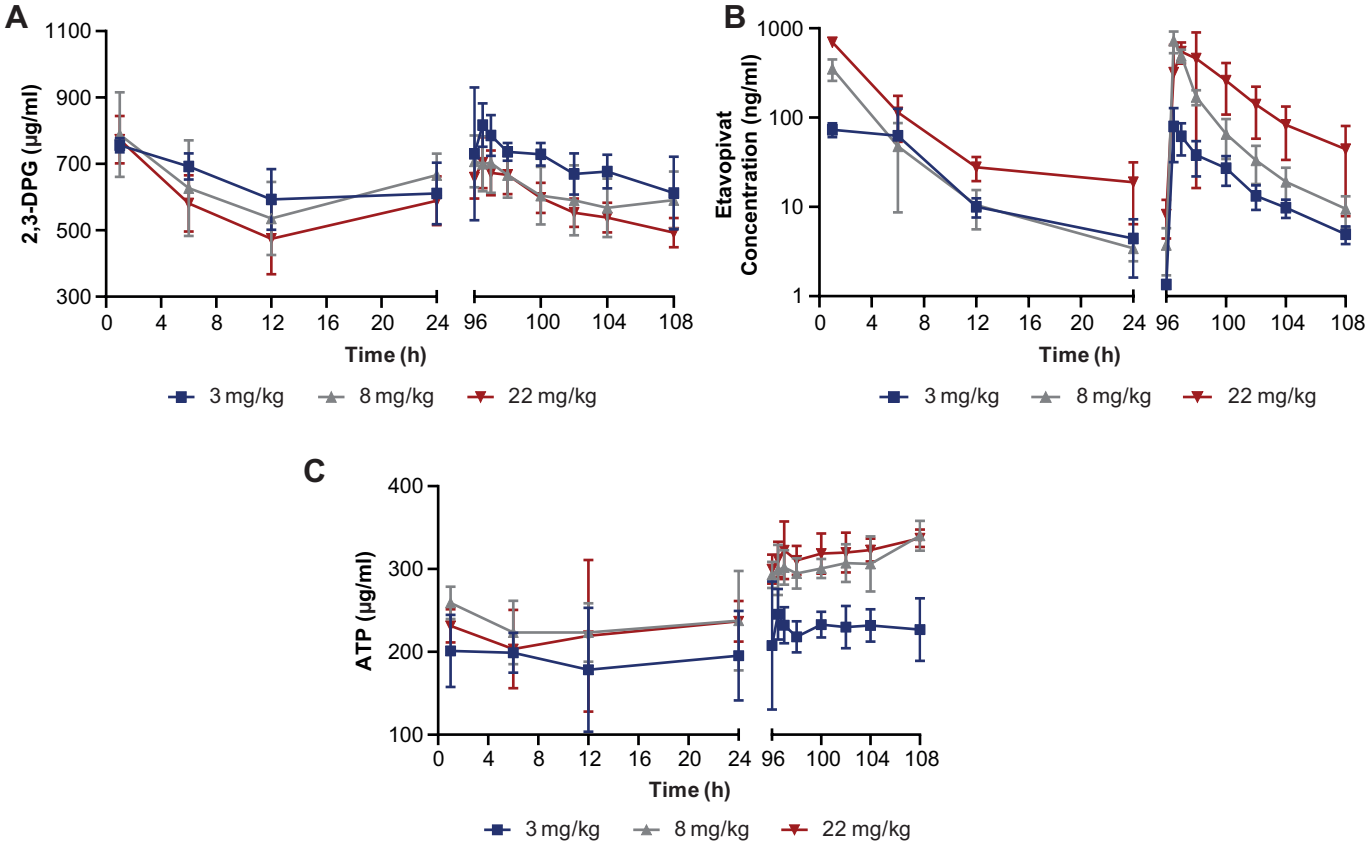
A
2,3-DPG (µg/ml)
1100
900
700
500
300
0 4 8 12 16 20 24 96 100 104 108
Time (h)
3 mg/kg
8 mg/kg
22 mg/kg
B
Etavopivat Concentration (ng/ml)
1000
100
10
1
0 4 8 12 16 20 24 96 100 104 108
Time (h)
3 mg/kg
8 mg/kg
22 mg/kg
C
ATP (µg/ml)
400
300
200
100
0 4 8 12 16 20 24 96 100 104 108
Time (h)
3 mg/kg
8 mg/kg
22 mg/kg

Figure 2

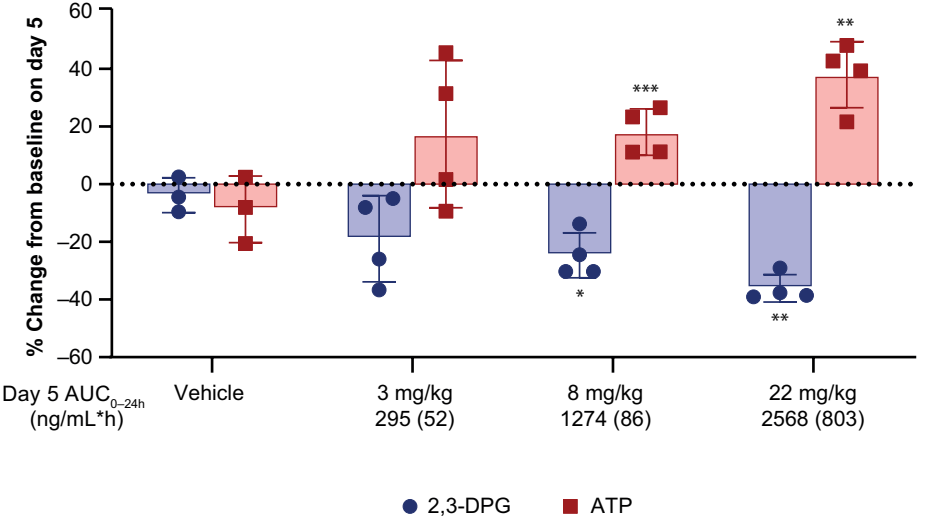
% Change from baseline on day 5
60
40
20
0
–20
–40
–60
***
**
*
**
Day 5 AUC0–24h (ng/mL*h)
Vehicle
3 mg/kg 295 (52)
8 mg/kg 1274 (86)
22 mg/kg 2568 (803)
2,3-DPG
ATP

Figure 3

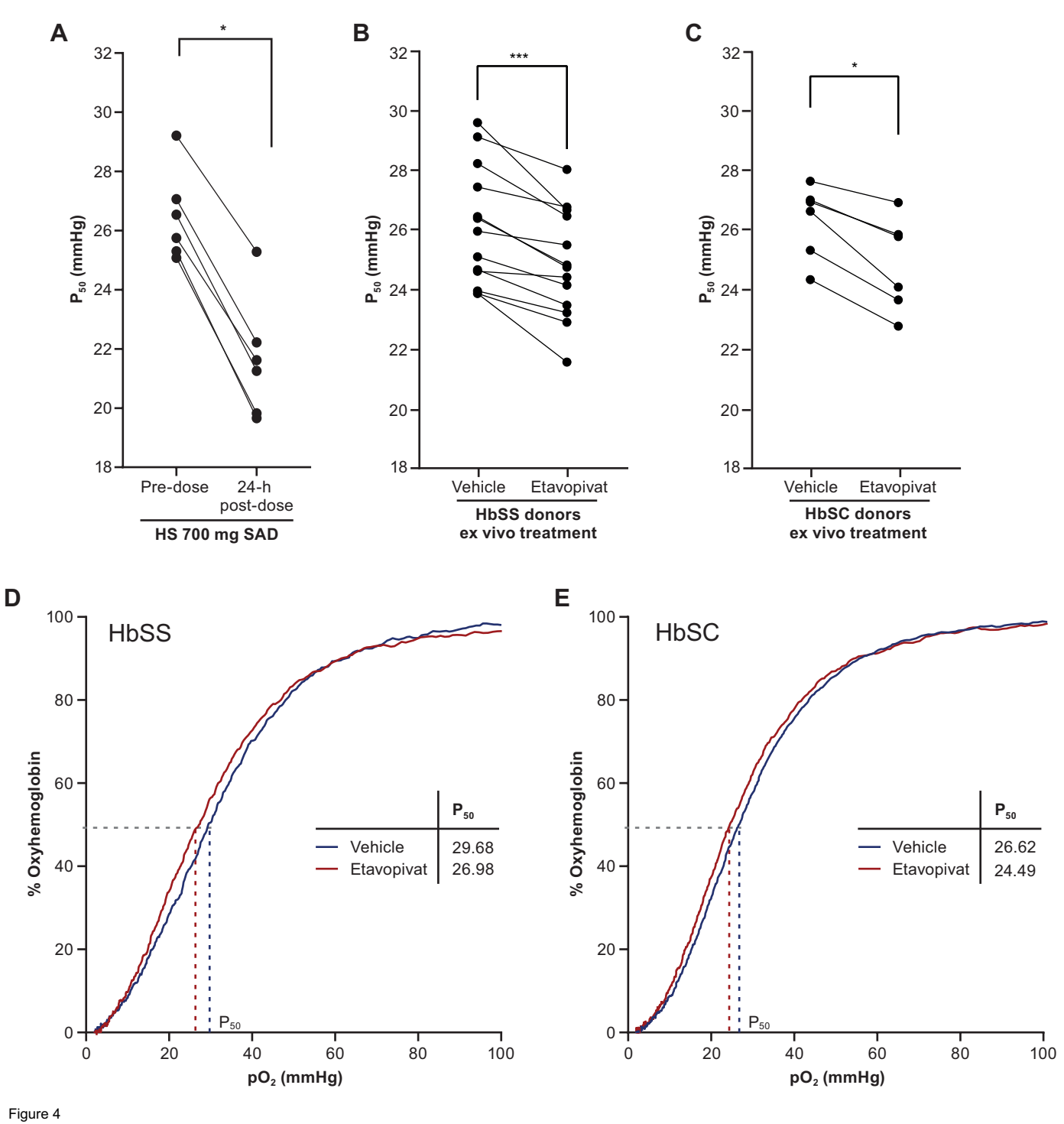
A
B
C
D
E
*
***
*
32
30
28
26
24
22
20
18
P50 (mmHg)
Pre-dose
24-h post-dose
HS 700 mg SAD
Vehicle
Etavopivat
HbSS donors ex vivo treatment
HbSC donors ex vivo treatment
HbSS
HbSC
100
80
60
40
20
0
% Oxyhemoglobin
pO2 (mmHg)
P50
Vehicle
Etavopivat
29.68
26.98
26.62
24.49

Figure 4

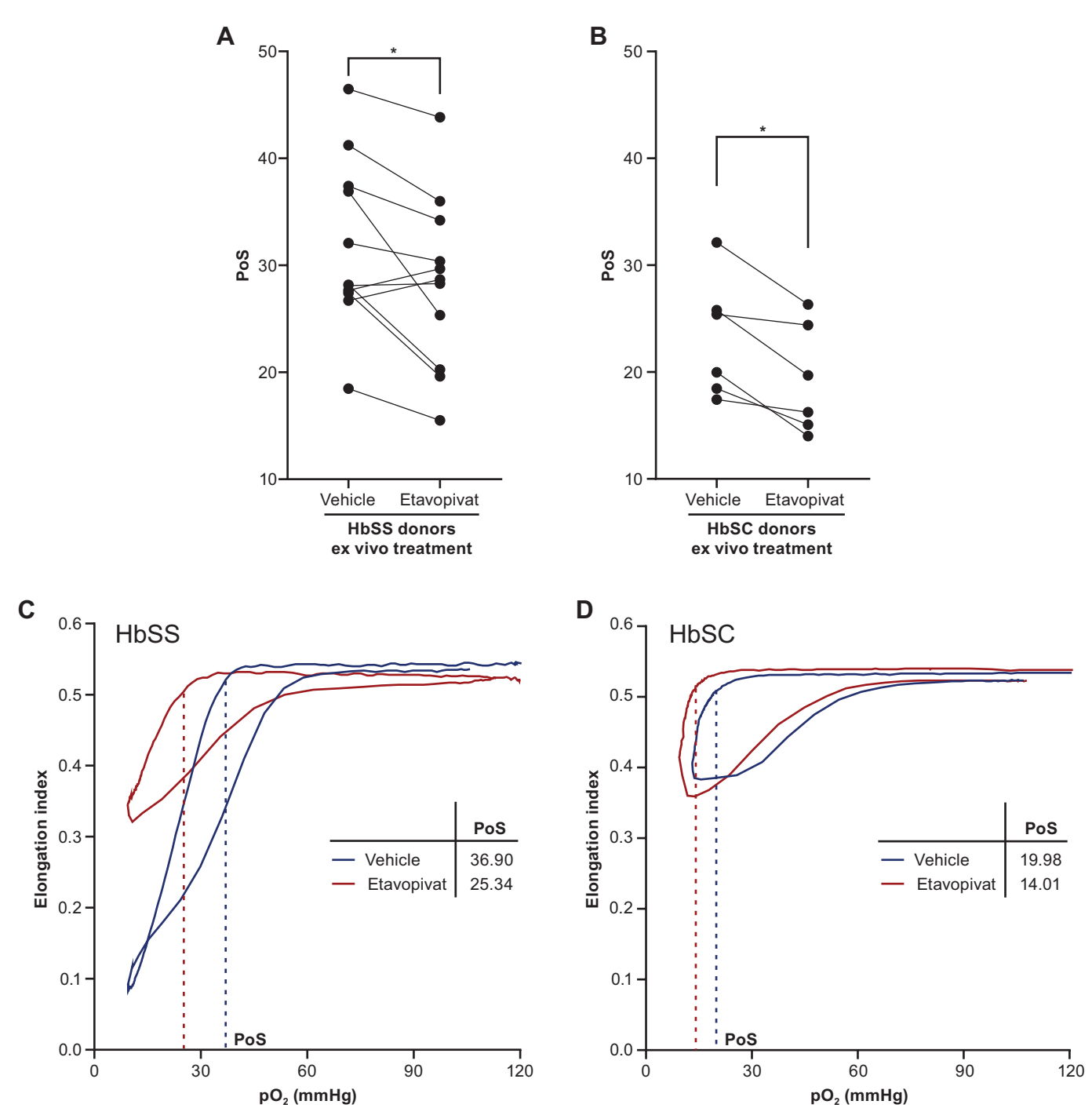
A
B
PoS
50
40
30
20
10
*
Vehicle
Etavopivat
HbSS donors
ex vivo treatment
HbSC donors
ex vivo treatment
C
D
HbSS
HbSC
Elongation index
0.6
0.5
0.4
0.3
0.2
0.1
0.0
0
30
60
90
120
pO2 (mmHg)
PoS
Vehicle
Etavopivat
36.90
25.34
19.98
14.01

Figure 5

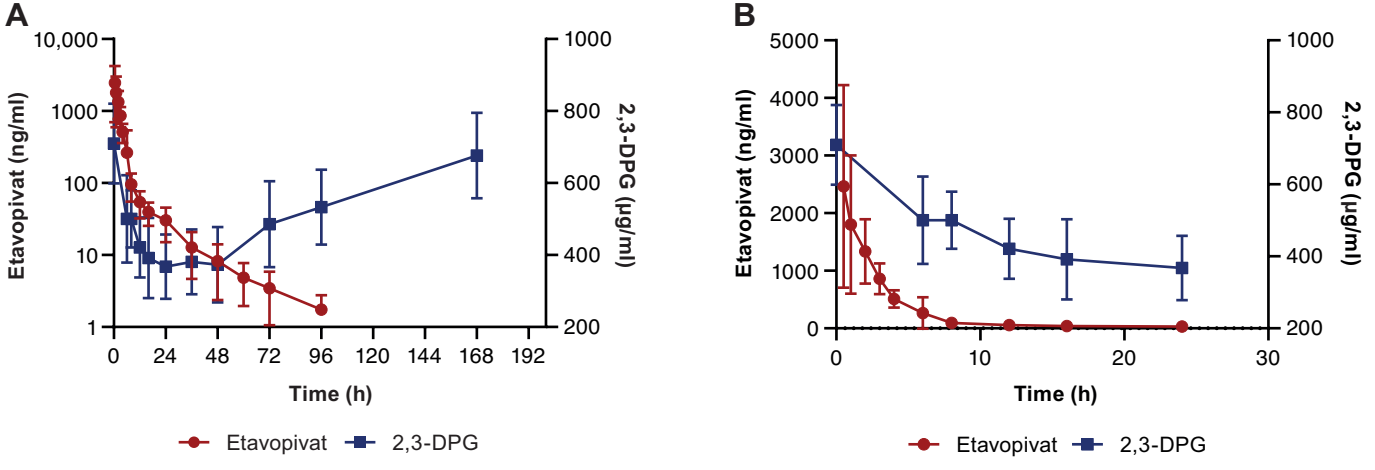
A
10,000
1000
100
10
1
Etavopivat (ng/ml)
1000
800
600
400
200
2,3-DPG (µg/ml)
0
24
48
72
96
120
144
168
192
Time (h)
Etavopivat
2,3-DPG
B
5000
4000
3000
2000
1000
0
Etavopivat (ng/ml)
1000
800
600
400
200
2,3-DPG (µg/ml)
0
10
20
30
Time (h)
Etavopivat
2,3-DPG

Figure 6

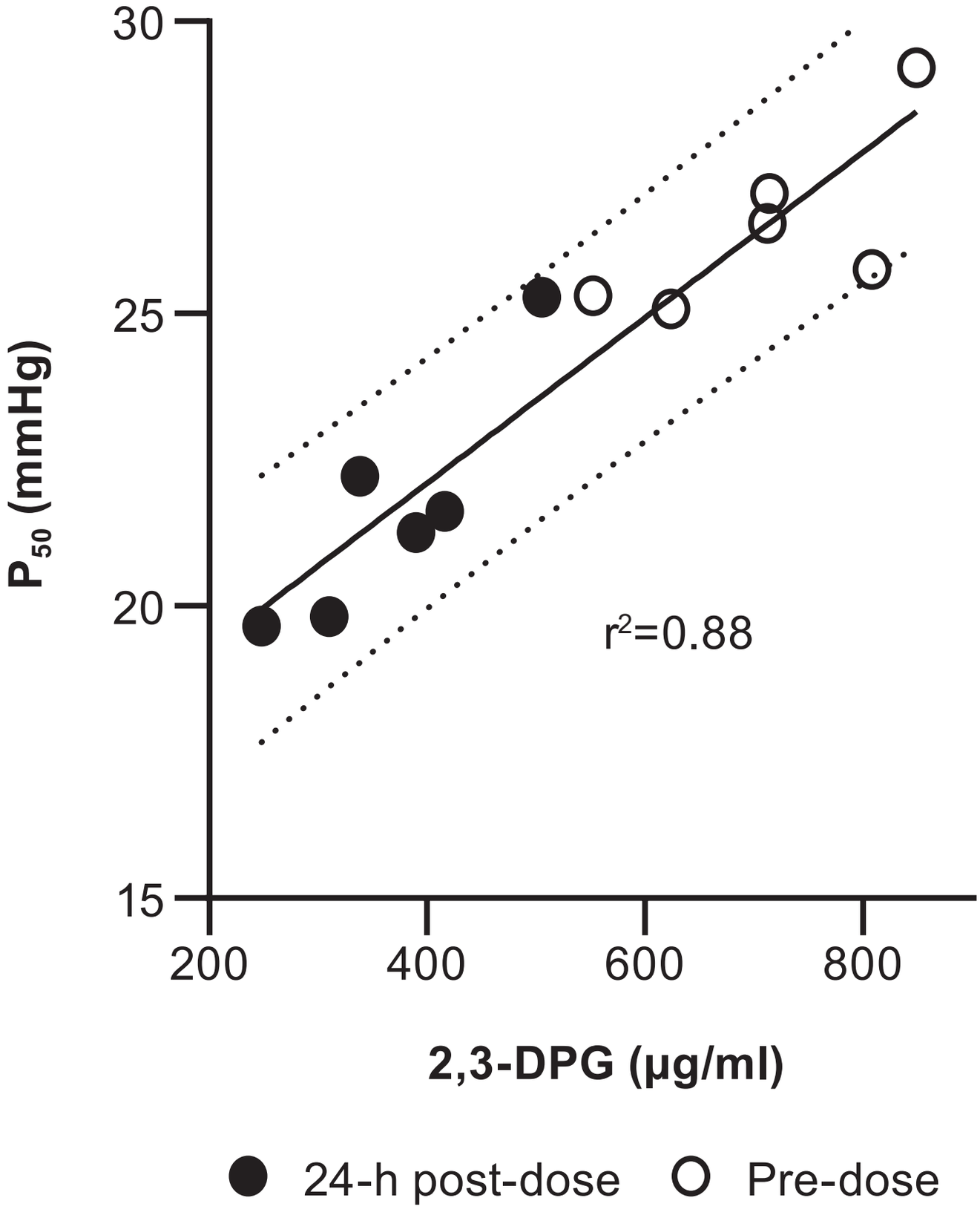
30
25
20
15
P_{50} (mmHg)
200
400
600
800
2,3-DPG (µg/ml)
r^2=0.88
24-h post-dose
Pre-dose

Figure 7

SUPPLEMENTAL DATA

Etavopivat, a Pyruvate Kinase Activator in Red Blood Cells, for the Treatment of Sickle Cell Disease

Patricia Schroeder,[1] Keertik Fulzele,[1] Sanjeev Forsyth, Maria D. Ribadeneira, Sylvie Guichard, Erik Wilker, C. Gary Marshall, Adam Drake, Rose Fessler, Diamantis G. Konstantinidis, Katie G. Seu, and Theodosia A. Kalfa

[1]*Co first authors*

Journal of Pharmacology and Experimental Therapeutics

JPET-AR-2021-000743

Text S1. 2,3-DPG PK/PD modeling

NHP PK and 2,3-DPG data were modeled using a simultaneous PK/PD approach utilizing Phoenix® NLME software (Certara, Princeton, NJ). The PK data were fit using a two-compartment model with first-order absorption. The 2,3-DPG data were fit using a basic indirect-response model (Dayneka et al., 1993; Sharma and Jusko, 1998) with a stimulation of loss function for 2,3-DPG shown in equation 1, where $2,3DPG_0$ is baseline 2,3-DPG levels, K_{out} is a first-order loss rate constant, S_{max} is the maximum ability of etavopivat to affect K_{out}, and SC_{50} is the etavopivat concentration resulting in 50% of the maximum stimulation achieved at the effect site.

$$\frac{d2,3DPG}{dt} = 2,3DPG_0 \cdot K_{out} - K_{out} \cdot \left(1 + \frac{S_{max} \cdot C}{C + SC_{50}}\right) \cdot 2,3DPG$$

The maximum 2,3-DPG suppression ($2,3DPG_{max}$) was estimated from equation 2.

$$2,3DPG_{max} = \left(\frac{2,3DPG_0}{1 + S_{max}}\right)$$

Half of the maximal 2,3-DPG response ($2,3DPG_{50}$) was estimated from equation 3

$$2,3DPG_{50} = 2,3DPG_0 - \frac{2,3DPG_0 - 2,3DPG_{max}}{2}$$

The plasma concentration resulting in half of the maximum decrease in 2,3-DPG (EC_{50}) was calculated using equation 4.

$$EC_{50} = \frac{SC_{50} \cdot (2,3DPG_0 - 2,3DPG_{50})}{2,3DPG_{50} \cdot (1 + S_{max}) - 2,3DPG_0}$$

Table S1. Etavopivat primary PK/PD parameters in non-human primates

Parameter	Value	S.D.
$2,3DPG_0$ (µg/mL)	841	9.79
K_{out} (h^{-1})	0.100	0.019
S_{max}	0.870	0.159
SC_{50} (ng/mL)	33.5	12.9

$2,3DPG_0$, baseline 2,3-DPG levels; K_{out}, first-order loss rate constant; PD, pharmacodynamic; PK, pharmacokinetic; S_{max}, maximum ability of etavopivat to affect K_{out}; SC_{50}, etavopivat concentration resulting in 50% of the maximum stimulation achieved at the effect site; S.D, standard deviation.

Table S2. Etavopivat exposure in non-human primates after single and repeated escalating doses

	Etavopivat mean (S.D.) PK parameters (oral dosing)			
	Day 1		Day 5	
Dose (mg/kg)	C_{max} (ng/ml)	$AUC_{0–24}$ (h·ng/ml)	C_{max} (ng/ml)	$AUC_{0–24}$ (h·ng/ml)
3	94 (44)	608 (292)	83 (45)	295 (52)
8	352 (95)	1116 (163)	725 (198)	1274 (86)
22	424 (320)	1728 (658)	689 (200)	2568 (803)
50	1823 (489)	8877 (1749)	ND	ND

n = 4 animals per dose

$AUC_{0–24}$, area under the concentration time curve from time 0–24 hours after dosing; C_{max}, maximum plasma concentration; ND, not determined; PK, pharmacokinetic; S.D, standard deviation.

Table S3. Change in P_{50} following etavopivat treatment in healthy subjects and ex vivo RBC from donors with SCD

	P_{50} Pre-dose (mmHg)	**P_{50} 24 hours post-dose (mmHg)**	**Change in P_{50} (mmHg)**
Healthy subjects: single 700-mg dose (*n* = 6)	26.5 (1.53)	21.6 (2.05)	4.85 (0.68)
	P_{50} - vehicle (DMSO) Treatment (mmHg)	**P_{50} - etavopivat Treatment (mmHg)**	**Change in P_{50} (mmHg)**
Ex vivo SCD RBC (HbSC disease) (*n* = 6)	26.3 (1.24)	24.8 (1.58)	1.47 (0.63)
Ex vivo SCD RBC (HbSS disease) (*n* = 13)	26.1 (1.99)	24.8 (1.82)	1.27 (0.76)

Data are mean (S.D.)

DMSO, dimethyl sulfoxide; P_{50}, the partial pressure of dissolved oxygen at which Hb is 50% saturated with oxygen; RBC, red blood cell; SCD, sickle cell disease; S.D., standard deviation.